

RESEARCH ARTICLE

Effect of changing the head position on accuracy of transverse measurements of the maxillofacial region made on cone beam computed tomography and conventional posterior-anterior cephalograms

¹Abbas Shokri, ²Amirfarhang Miresmaeili, ²Nasrin Farhadian, ³Sepideh Falah-kooshki, ⁴Payam Amini and ⁵Najmeh Mollaie

¹Department of Oral and Maxillofacial Radiology, Faculty of Dentistry, Dental Research Center, Hamadan University of Medical Sciences, Hamadan, Islamic Republic of Iran; ²Department of Orthodontics, Faculty of Dentistry, Dental Research Center, Hamadan University of Medical Sciences, Hamadan, Islamic Republic of Iran; ³Department of Oral and Maxillofacial Radiology, Faculty of Dentistry, Kermanshah University of Medical Sciences, Kermanshah, Islamic Republic of Iran; ⁴Department of Epidemiology and Reproductive Health, Reproductive Epidemiology Research Center, Royan Institute for Reproductive Biomedicine, ACECR, Tehran, Islamic Republic of Iran; ⁵Department of Orthodontics, Faculty of Dentistry, Rafsanjan University of Medical Sciences, Rafsanjan, Islamic Republic of Iran

Objectives: This study aimed to assess the effect of head position on the accuracy of transverse measurements of the maxillofacial region on CBCT and conventional posterior-anterior (PA) cephalograms. The second objective of this study was to find skull positions with the greatest and smallest effect on transverse measurements in the maxillofacial region.

Methods: PA cephalograms and CBCT scans were obtained from 10 dry human skulls in 7 positions, namely the central position, 10° and 20° rotations, 10° and 20° tilts and 10° and 20° tips. The CBCT scans were converted to PA cephalograms on which distances from six landmarks, namely the nasal cavity, zygomatic arch, jugale, antegonion, condyion and zygomaticofrontal suture to the mid-sagittal plane, were measured on both sides using Dolphin two-dimensional software. The paired *t*-test was used to compare the mean values separately in each position (for each landmark) with the gold standard (central skull position). The interclass correlation coefficient and the Bland–Altman plot were used to compare the mean values measured by two observers.

Results: The mean values of the distances measured on CBCT PA cephalograms were greater than those measured on conventional PA cephalograms; this difference was statistically significant for some landmarks ($p < 0.005$). The rotated position (as compared with the central position) caused the greatest change in values for most landmarks on both sides ($p < 0.005$).

Conclusions: The CBCT PA cephalogram was more accurate than the conventional PA cephalogram, and landmarks farther from the midline exhibited greater changes on cephalograms compared with those closer to the midline. Patients are at risk of improper positioning when undergoing extraoral radiography such as PA cephalograms. Changes in head position may affect the transverse measurements and thus the treatment plan.

Dentomaxillofacial Radiology (2017) **46**, 20160180. doi: 10.1259/dmfr.20160180

Cite this article as: Shokri A, Miresmaeili A, Farhadian N, Falah-kooshki S, Amini P, Mollaie N. Effect of changing the head position on accuracy of transverse measurements of the maxillofacial region made on cone beam computed tomography and conventional posterior-anterior cephalograms. *Dentomaxillofac Radiol* 2017; **46**: 20160180.

Keywords: cephalometry; CBCT

Introduction

Success of orthodontic treatment highly depends upon the ability of the clinician to comprehend the relationship of dental structures, soft tissues and bone. Lateral and frontal cephalometric radiographs have been used for maxillofacial analyses, evaluation of orthodontic deformities and monitoring growth and development since the early 1930s.^{1,2} Nowadays, cephalograms are routinely requested by clinicians for accurate diagnosis and treatment planning.³ Although posteroanterior (PA) cephalometry is not commonly requested by many orthodontists, it provides valuable information for quantitative and qualitative analyses of the craniofacial region especially for the diagnosis of transverse discrepancies and asymmetries. Also, PA cephalometry is used for the diagnosis of craniofacial anomalies and dentoskeletal asymmetries and for determining the pattern of transverse growth of the maxilla and mandible.^{3,4} The limitations and shortcomings of this modality include image superimposition, image distortion and difficulty in identification of landmarks.^{5,6} Other problems include difficult standardization and reproducibility of head repositioning and maintaining a fixed distance between the film and the object.⁷⁻⁹

CT was introduced in 1972 and quickly gained popularity for orthodontic diagnosis and treatment planning.^{10,11} However, conventional CT has shortcomings such as high cost and relatively high patient radiation dose.¹⁰ CBCT was introduced for dentistry in 1988, and it is currently an ideal imaging modality for many dental applications.¹² This modality has superiority over conventional CT mainly owing to having a lower patient radiation dose, lower cost and higher spatial resolution. CBCT also enables reconstruction of two-dimensional (2D) views from three-dimensional (3D) images for conventional cephalometric analysis.¹² The ray sum technique is used to convert CBCT scans to 2D PA cephalograms.¹² Cephalograms obtained from CBCT scans by the use of the ray sum technique do not have the distortion of conventional cephalograms. However, the use of 2D cephalograms obtained from CBCT scans as an alternative to conventional cephalograms has yet to be established.

According to the 2007 recommendations of the International Commission on Radiological Protection Publication 103 for calculation of effective dose, the three routinely used radiographic modalities in orthodontics include lateral cephalometry, PA cephalometry and panoramic radiography with a collective effective dose of 25–35 μ Sv, whereas the effective dose of CBCT with a large field of view used for orthodontic diagnosis ranges from 68 μ Sv to 1073 μ Sv, which is several times higher than the total dose of lateral cephalometry, PA cephalometry and panoramic radiography.¹² Diagnostic information obtained from CBCT improves the outcome of treatment, shortens the course of recovery and decreases the treatment cost; thus, these advantages

may compensate for the higher patient radiation dose. However, despite these advantages, this technique is not recommended. Taking patient radiation dose into account, conventional PA cephalometry is preferred to CBCT. CBCT is an ideal modality for complex cases requiring a thorough evaluation of the temporomandibular joint or other 3D structures prior to surgery because it provides more information than cephalometry and significantly enhances diagnosis and treatment planning, which may justify its use despite higher radiation dose.¹³

In most extraoral radiographies such as lateral and PA cephalometric radiographs, patients are at risk of improper positioning. CBCT scans are less commonly affected by improper patient positioning; however, during the process of image acquisition, maintaining a fixed position of the skull is necessary.⁷ Previous studies showed that rotation of the head significantly affects the accuracy of transverse measurements in the maxillofacial region, while tilting the head has no effect on the accuracy of transverse measurements in this region.^{14,15} To the best of the authors' knowledge, no previous study has evaluated the effect of tilting, rotation or tipping of the skull on the accuracy of transverse analysis of the maxillofacial region on CBCT and PA cephalograms. Thus, this study aimed to assess the effect of head position on the accuracy of landmark detection and transverse analysis of the maxillofacial region. The second objective was to find skull positions with the greatest and smallest effects on the accuracy of transverse analysis. The effects of head position on the accuracy of transverse measurements made on CBCT and PA cephalograms were also assessed.

Methods and materials

This study was conducted on dry human skulls. The study protocol was approved by the Medical Ethics Committee of the Hamadan University of Medical Sciences (ethical approval code: Res:project:9303191154). 10 dry skulls without asymmetry, fracture or pathologic lesions were selected for this study. The condyles were placed in the glenoid fossae in order to fix the mandible to the maxilla during image acquisition; Sticky wax (Kerr, Orange, CA) was melted at 73 °C (163 °F);^{16,17} 1–5 mm of sticky wax was placed between the maxillary and mandibular teeth and 5–10 mm of sticky wax was placed between the maxillary and mandibular ridges in edentulous areas.

Positions

Skulls were adjusted in the central and six other positions, namely 10° rotation, 20° rotation, 20° tilt, 10° tilt, 20° tip and 10° tip, and conventional PA and CBCT PA cephalograms were obtained. Owing to differences in anatomical dimensions of the right and left sides of each

skull, tilts and rotations of the skulls were applied to one side only.

Central position: The skulls were placed in the standard position. [Figure 1](#) shows the conventional PA cephalograms and the CBCT PA cephalograms of the skulls in central position.

Tilted position: The mid-sagittal plane of the skulls was tilted to the right side. [Figure 2](#) shows the conventional PA cephalograms and the CBCT PA cephalograms of the skulls tilted towards the right by 20°.

Rotated position: The skulls were rotated to the right side. [Figure 3](#) shows the conventional PA cephalograms and the CBCT PA cephalograms of the skulls rotated to the right side by 20°.

Tipped position: The skulls were tipped downwards. [Figure 4](#) shows the conventional PA cephalograms and the CBCT PA cephalograms of the skulls tipped downwards by 20°.

Conventional posteroanterior cephalometry protocol

Conventional PA cephalograms were obtained by a Scara II Planmeca X-ray unit (Planmeca, Helsinki, Finland) with exposure settings of 68 kVp, 10 mA and 15.3 s. Each skull was placed on a styrofoam sheet, and the mandible was outlined on the sheet. The outlined area was cut out of the sheet and the mandible was placed in the created space. Mandibles were positioned in styrofoam sheets such that the Frankfurt plane of the skull was parallel to the horizon.

A wooden apparatus was designed and fabricated for positioning of the skulls for conventional PA cephalometry with a height of 120 cm. Two wooden sheets were placed on the upper part of the apparatus, and the inferior wooden sheet had a screw by which the position (angulation) of the skull could be adjusted. Next, each skull along with the respective styrofoam sheet was placed on the wooden apparatus.

In conventional PA cephalometry, a cephalostat was used to fix the position of the skull relative to the detector and X-ray tube. Using a cephalostat, the distance between the mid-sagittal plane of the skull and detector and also the distance between the mid-sagittal plane and X-ray tube remained constant. It also enabled reproducibility of PA cephalometry in correct position.¹⁴

On conventional PA cephalogram in central position, each skull was adjusted in standard position ([Figure 5a](#)) such that the petrous ridge of the temporal bone was superimposed on the maxillary sinus floor ([Figure 1](#)).

In order to position the skulls in 10° and 20° tilted position, the skulls were first adjusted in central position and PA cephalograms were taken. After confirming central position of the skull, 10° and 20° angles were created between the two superior sheets of the wooden apparatus, and the skull was tilted to the right side by 10° and 20°, respectively ([Figure 5b](#)).

For the rotation position, the skulls were first placed in central position and PA cephalograms were obtained from them. After confirming central position of the skull, the wooden apparatus was rotated 10° and 20° to the right and a PA cephalogram was obtained in this position ([Figures 5c](#) and [6](#)). As shown in [Figure 6](#), the wooden apparatus was rotated 20° to the right (90° from its baseline). The skull (previously in central position) was also rotated along with the apparatus to the right and the PA cephalogram was taken.

For the tipping position, after confirming the central position of the skull, 10° and 20° angles were created between the two superior sheets of the wooden apparatus and the skull was tipped downwards ([Figure 5d](#)).

The CBCT protocol

The CBCT scans were obtained by a NewTom 3G volume scanner (QR SRL, Verona, Italy) with exposure settings of 110 kVp, 2.8 mA, 3.6 s and 12-inch field of view. The scans were processed using NNT Viewer software (QR SRL, Verona, Italy). The skulls were

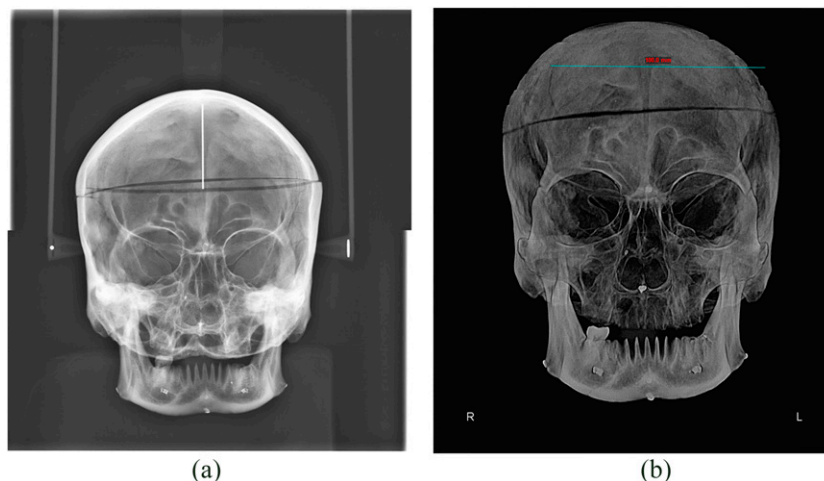


Figure 1 Taking conventional posteroanterior (PA) cephalograms (a) and CBCT PA cephalograms (b) of the skulls in the central position.

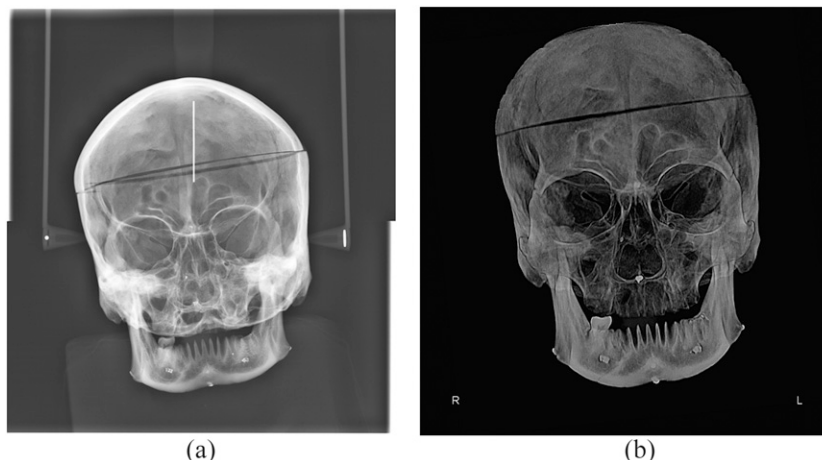


Figure 2 Taking conventional posteroanterior (PA) cephalograms (right) and CBCT PA cephalograms (left) of the skulls tilted towards the right side by 20°.

placed in central and six other positions mentioned earlier.

In order to obtain CBCT scans, the position of the skulls had to be fixed. For this purpose, each skull was placed on a styrofoam sheet and outlined. The outlined area was cut out of the styrofoam sheet. Each skull was placed in its respective styrofoam sheet for scanning (Figure 7).

In central position, laser light of the CBCT unit was adjusted to the mid-sagittal plane of the skull. The Frankfurt plane of the skull was perpendicular to the horizon, and CBCT scans were obtained in this position (Figure 7a). To obtain CBCT scans in the tilted position, skulls were first placed in central position. After confirming the central position of each skull, the skulls were tilted by 10° and 20°. As shown in Figure 8, the mid-sagittal plane of the skull in central position was considered as the reference plane, and then the skull was tilted to the right by 20° (corresponding to the dotted line) (Figure 7b).

To obtain CBCT scans in rotation, the skulls were first placed in the central position. After confirming, the skulls were rotated by 10° and 20° (Figure 7c). Triangular wedges measuring 4 × 20 × 25 mm and 8 × 20 × 25 mm and tapered by 10° and 20° towards their tip were placed beneath the styrofoam sheet from the left side, and images were captured.

To obtain CBCT scans in tipped position, after confirming the central position of each skull on CBCT scans, triangular wedges were placed beneath the styrofoam sheet and the skulls were tipped downwards by 10° and 20° (Figure 7d).

Image evaluation

The PA cephalograms were obtained from CBCT images. The steps taken to obtain a CBCT PA cephalogram in NewTom 3G are as follows: image creation, new 3D model, load 3D and ray cast model style. On conventional and CBCT PA cephalograms taken at seven different positions, the distance from each of the

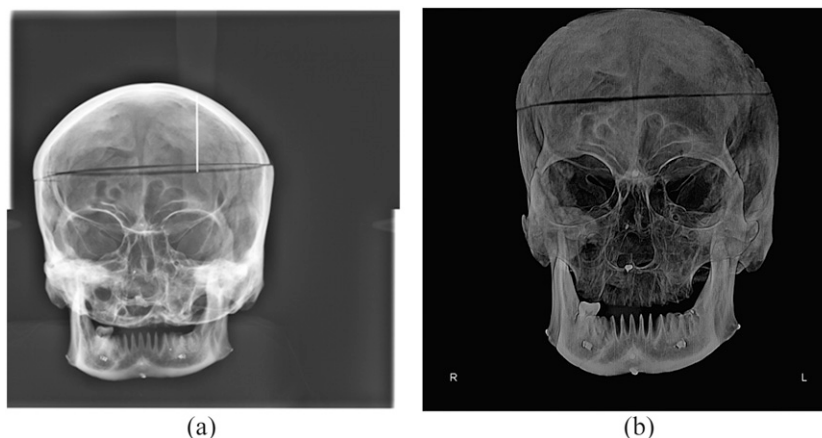


Figure 3 Taking conventional posteroanterior (PA) cephalograms (a) and CBCT PA cephalograms (b) of the skulls rotated to the right side by 20°.



Figure 4 Taking conventional posteroanterior (PA) cephalograms (a) and CBCT PA cephalograms (b) of the skulls tipped downwards by 20°.

below-mentioned landmarks to the mid-sagittal plane was measured using Dolphin 2D software v. 11.7 (Chatsworth, CA).

- Jugale (J): the intersection point of outline of the maxillary tuberosity and zygomatic buttress in the right and left sides
- Antegonion (AG): the notch at the inferolateral margin of AG protuberance in the right and left sides
- Zygomaticofrontal suture: the cranial suture between the frontal and zygomatic bones
- Zygomatic arch: this is formed by the zygomatic process of the temporal bone.

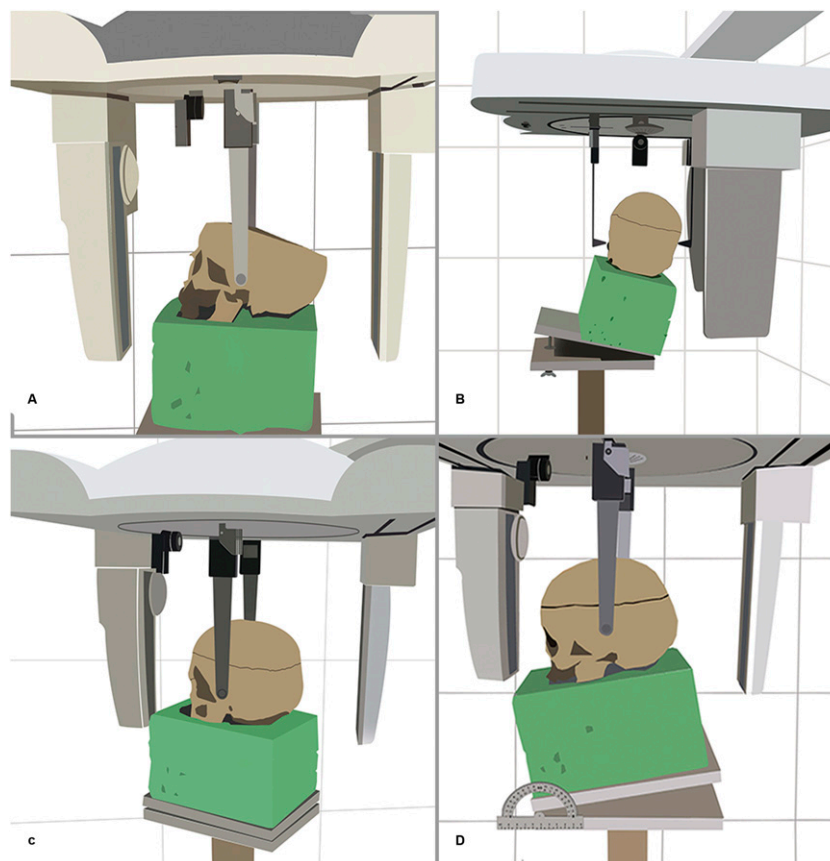


Figure 5 Taking conventional posteroanterior cephalograms of the skulls in central position (a), tilted position (b), rotated position (c) and tipped position (d).

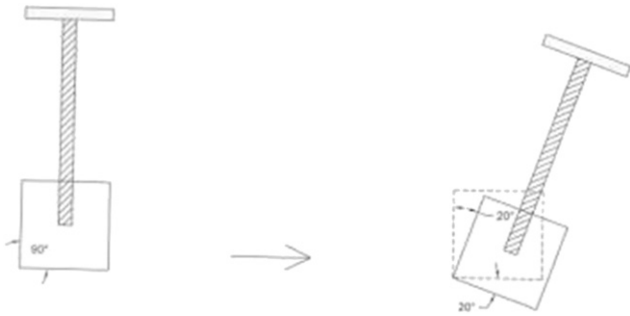


Figure 6 A schematic view of the rotation of the wooden apparatus by 20° relative to the central position for taking conventional posteroanterior cephalograms in the 20° rotated position.

- Width of nasal pyriform: nasal cavity at the widest point
- Condylion: this is the most lateral point of the mandible in the glenoid fossa of the temporal bone.

Figure 9 shows the schematic view and PA cephalogram of transverse distances between the zygomatico-frontal suture, zygomatic arch, condylion, jugale, nasal cavity and antegonion landmarks.

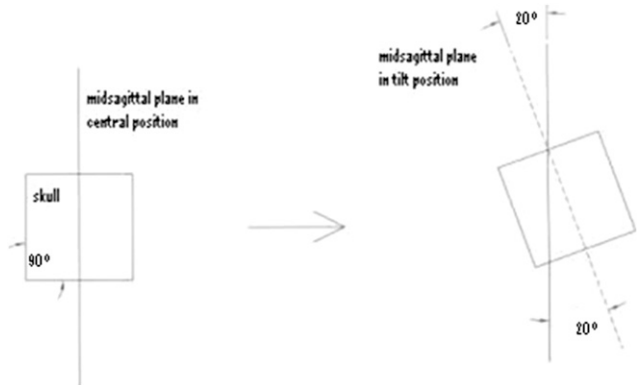


Figure 8 A schematic view of the tilted position of the skull by 20° relative to the central position to take CBCT scans in the 20° tilted position.

Statistical analysis

On conventional and CBCT PA cephalograms, the central position of skulls 1–10 was considered as the gold standard, and the distances measured in other positions were compared with the gold standard values. Transverse measurements made in tilted, rotated and tipped positions were compared with the transverse distances measured in the central position of the skulls

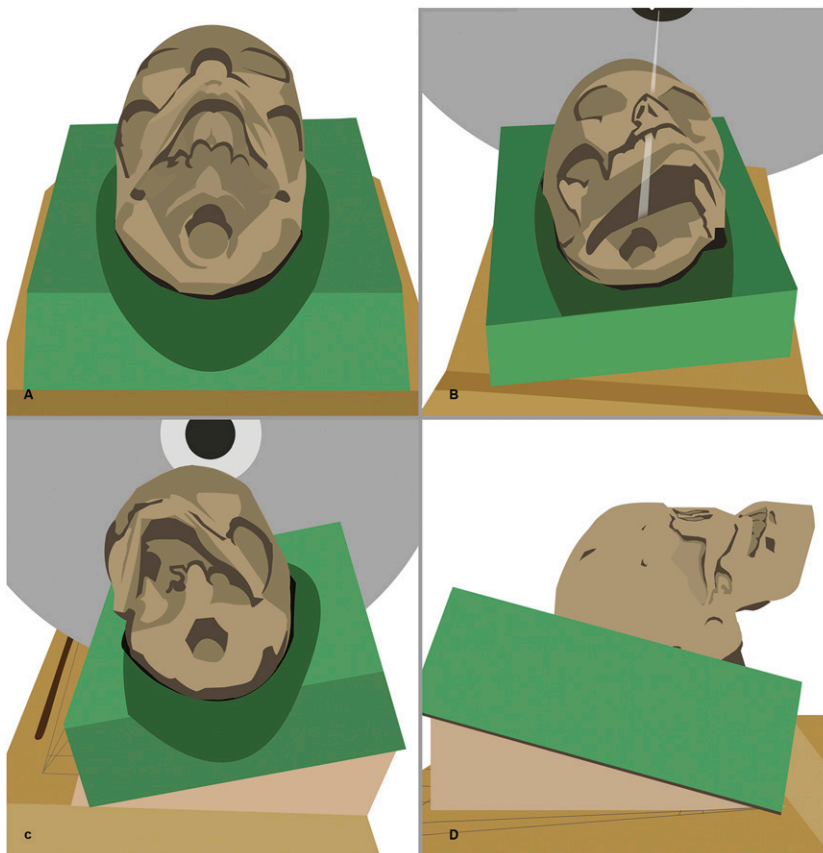


Figure 7 Taking CBCT scans of the skulls in central position (a), tilted position (b), rotated position (c) and tipped position (d).

(for each landmark). The paired *t*-test was used to compare the mean values for each position (separately for each landmark) with the gold standard values. All statistical analyses were performed using SPSS® v. 12 (IBM Corp., New York, NY; formerly SPSS Inc., Chicago, IL) and R software v. 3.0.2 (random effects model and Bootstrap model; University of Auckland, New Zealand) with 95% confidence interval. Also, the interclass correlation coefficient and the Bland–Altman plot were used to compare the mean values measured by the two observers. Observations were made by two experienced observers. The first observer was an oral and maxillofacial radiologist and the second observer was an orthodontist. Each observer made the measurements independently. 2 weeks later, all measurements were repeated by the two observers.

Results

For the conventional and CBCT PA cephalograms, central positions of the 10 skulls were considered as the gold standard. The mean values of the distances in the right and left sides of the 10 skulls in 10° tilted position were independently calculated and compared with the mean distances of the right and left sides on PA cephalograms of the 10 skulls in central position. This was repeated for other positions as well. The results are presented in Tables 1 and 2. Based on the results presented in Tables 1 and 2, changes in transverse distances between landmarks in tested positions of the skulls relative to the central position were evaluated.

In our study, on both conventional and CBCT cephalograms, the mean distances from different landmarks to the mid-sagittal plane in tilted and rotated positions were smaller than those in the central position on the right side and greater than those in the central position on the left side. Since tilting and rotation of skulls were towards the right, the values measured in this position on the right were smaller than the values measured in the central position. The opposite was true for the left side. The changes in 20° tilted and rotated positions compared with the central position were greater than those in 10° tilted and rotated positions. The rotated position affected the mean values more than the tilted position. The mean distances measured in tipped position were the closest to the mean values measured in central position. In the tipped position, the mean distances measured were greater than those measured in the central position (and had an ascending trend). These changes in 20° tipped position were greater than those in 10° tipped position.

Next, the mean distances on the right and left sides of the 10 skulls in central position on conventional PA cephalograms (gold standard) were compared with those on CBCT PA cephalograms of the 10 skulls. The results are presented in Table 3. As shown in Table 3, the mean values of distances measured on CBCT PA cephalograms were greater than those measured on

conventional PA cephalograms, and the difference in this regard was significant for some landmarks ($p < 0.05$).

The Bootstrap simulation method was conducted to assess the difference in standard deviation (SD) of central position on conventional and CBCT PA cephalograms.

The results are shown in Table 4. As presented in Table 4, the difference in the SDs of the mean distances of different landmarks in central position was not significant between conventional and CBCT PA cephalograms. Since there was no significant difference in the SDs of the two modalities, the mean values obtained in central position were compared between the two methods.

Changes in measurements of different landmarks in tilted, rotated and tipped positions (compared with the central position) were compared between conventional and CBCT PA cephalograms. Table 5 shows significant changes in this regard between the two modalities. As demonstrated in Table 5, significant differences were noted for most landmarks in measurements made on conventional and CBCT PA cephalograms in 10° and 20° rotations compared with the central position at both sides.

To assess the interobserver agreement in conventional and CBCT PA cephalometry, interclass correlation coefficient was applied and the Bland–Altman plot was drawn for the items with the highest and lowest significance. The results are presented in Figures 10 and 11. Figure 10 shows a high interobserver agreement for AG measurements in the tilted position by 20° on a conventional PA cephalogram. Figure 11 shows a low interobserver agreement for zygomatic arch measurements in tipping by 10° on the left side on the conventional PA cephalogram.

Discussion

PA cephalometry provides valuable information about the asymmetries and horizontal jaw relations. Data obtained from PA cephalograms are of high clinical significance in patients requiring surgical interventions.² Also, CBCT is requested for patients with 3D deformities such as craniofacial anomalies or orofacial clefts. Evidence shows that conventional lateral cephalograms may be comparable with CBCT cephalograms.^{18–20} Use of CBCT-generated lateral and PA cephalograms has greatly increased in the recent years and has become a routine in diagnostic CBCT report of patients undergoing orthodontic treatment.¹²

In the present study, dry skulls were used because patient exposure by both conventional radiography and CBCT was not ethically feasible. This study aimed to assess the effect of head position on skeletal landmark detection and transverse analysis on PA cephalograms. Thus, soft tissues were not simulated in order to allow better visualization of skeletal landmarks and prevent

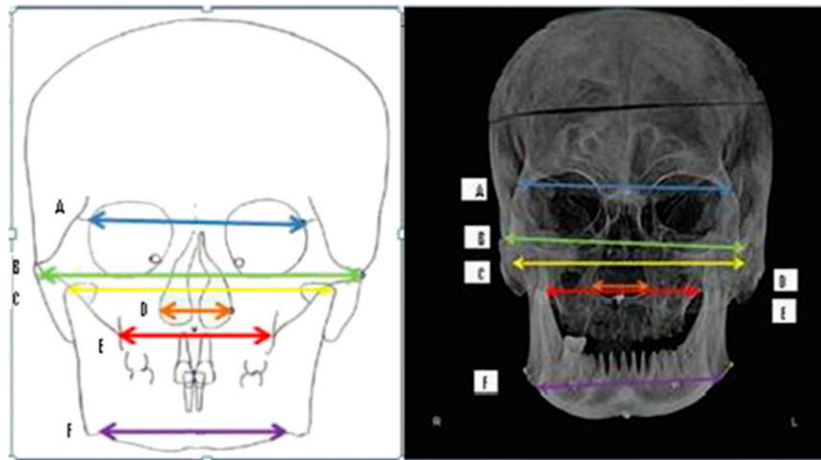


Figure 9 Transverse distances between landmarks: (A) zygomaticofrontal suture–zygomaticofrontal suture, (B) zygomatic arch–zygomatic arch, (C) condyilion–condyilion, (D) nasal cavity–nasal cavity, (E) jugale (J)–J, (F) antegonion (AG)–AG.

image distortion. As a result, errors in detection of landmarks decreased, and skeletal landmarks were more easily and accurately identified and traced. Landmark selection in each analysis depends on the objective of the respective analysis.²¹ The highest error in cephalometric studies is related to landmark identification. Identification of points at the intersections of two lines is by far easier than that of those on wide arches. The J landmark is located at the intersection of the maxillary tuberosity and zygomatic buttress, but AG is located on a wide arch.^{22–24}

The slice thickness of orthogonal or multiplanar reformatted images can be “thickened” by increasing the number of adjacent voxels in the display. This results in an image slab representing a specific volume of the patient, referred to as a ray sum. The slab thickness is often variable and is determined by the thickness of the structure to be imaged. Full-thickness perpendicular ray sum images can be used to generate simulated projections, such as lateral cephalometric images. This technique uses the entire volumetric data set, and interpretation is negatively affected by “anatomic noise”, the superimposition of

Table 1 Comparison of measurements made in tilted, rotated and tipping positions with those made in central position on conventional posteroanterior cephalograms separately for each landmark (in mm)

Position	Central		Tilt 10°		Tilt 20°		Central		Tilt 10°		Tilt 20°	
	Side	R	R	R	R	L	L	L	L	L	L	
PAC	Mean ± SD	Mean ± SD	p-value	Mean ± SD	p-value	Mean ± SD	Mean ± SD	p-value	Mean ± SD	Mean ± SD	p-value	
AG	39.46 ± 4.87	37.76 ± 4.27	0.019	37.40 ± 3.89	0.026	41.72 ± 3.74	43.17 ± 3.87	0.078	43.87 ± 3.98	0.021		
J	28.24 ± 2.58	27.77 ± 2.71	0.589	27.26 ± 2.46	0.214	28.98 ± 3.11	29.68 ± 2.73	0.281	29.69 ± 2.68	0.239		
ZA	53.65 ± 1.74	53.40 ± 1.52	0.512	53.37 ± 1.55	0.627	54.52 ± 1.68	54.71 ± 1.53	0.704	54.87 ± 1.72	0.576		
NC	11.12 ± 1.51	10.82 ± 1.55	0.341	10.47 ± 1.64	0.171	12.84 ± 2.29	12.84 ± 1.45	1.00	12.94 ± 2.43	0.856		
ZF	50.22 ± 1.11	49.80 ± 0.90	0.445	49.78 ± 1.04	0.339	49.91 ± 1.04	50.24 ± 1.10	0.493	50.26 ± 1.10	0.384		
CO	52.57 ± 2.98	51.80 ± 2.69	0.410	50.47 ± 1.93	0.022	54.25 ± 4.19	55.96 ± 4.15	0.103	56.34 ± 4.08	0.023		
Position	Central	Rotation 10°	p-value	Rotation 20°	p-value	Central	Rotation 10°	p-value	Rotation 20°	p-value		
Side	R	R		R		L	L		L			
PAC	Mean ± SD	Mean ± SD		Mean ± SD		Mean ± SD	Mean ± SD		Mean ± SD			
AG	39.46 ± 4.87	36.22 ± 6.22	0.027	34.36 ± 8.10	0.008	41.72 ± 3.74	44.73 ± 4.51	0.023	48.29 ± 3.95	0.001		
J	28.24 ± 2.58	27.43 ± 2.22	0.429	26.29 ± 3.57	0.157	28.98 ± 3.11	30.21 ± 4.20	0.245	30.70 ± 4.31	0.142		
ZA	53.65 ± 1.74	51.06 ± 2.14	0.012	50.07 ± 2.10	0.003	54.52 ± 1.68	56.45 ± 2.90	0.102	57.36 ± 2.05	0.007		
NC	11.12 ± 1.51	10.29 ± 1.86	0.224	9.34 ± 2.46	0.085	12.84 ± 2.29	12.92 ± 1.76	0.915	13.24 ± 2.95	0.675		
ZF	50.22 ± 1.11	49.02 ± 1.63	0.052	48.77 ± 1.17	0.030	49.91 ± 1.04	50.64 ± 1.32	0.083	50.81 ± 2.37	0.259		
CO	52.57 ± 2.98	47.32 ± 5.15	0.025	42.79 ± 6.97	0.000	54.25 ± 4.19	61.14 ± 6.10	0.002	64.68 ± 7.01	0.000		
Position	Central	Tip 10°	p-value	Tip 20°	p-value	Central	Tip 10°	p-value	Tip 20°	p-value		
Side	R	R		R		L	L		L			
PAC	Mean ± SD	Mean ± SD		Mean ± SD		Mean ± SD	Mean ± SD		Mean ± SD			
AG	39.46 ± 4.87	40.33 ± 5.30	0.096	41.19 ± 5.11	0.031	41.72 ± 3.74	41.78 ± 3.24	0.926	42.79 ± 3.56	0.038		
J	28.24 ± 2.58	28.27 ± 2.82	0.968	28.31 ± 3.16	0.944	28.98 ± 3.11	29.16 ± 1.81	0.737	29.56 ± 2.54	0.380		
ZA	53.65 ± 1.74	53.65 ± 1.65	1.000	53.72 ± 2.32	0.933	54.52 ± 1.68	54.52 ± 1.68	0.759	55.27 ± 1.61	0.322		
NC	11.12 ± 1.51	11.13 ± 1.42	0.981	11.21 ± 0.76	0.821	12.84 ± 2.29	12.89 ± 1.82	0.928	13.04 ± 1.27	0.678		
ZF	50.22 ± 1.11	50.28 ± 0.44	0.910	50.31 ± 1.00	0.842	49.91 ± 1.04	50.08 ± 0.84	0.614	50.13 ± 0.87	0.564		
CO	52.57 ± 2.98	52.62 ± 2.77	0.944	52.77 ± 4.29	0.868	54.25 ± 4.19	54.47 ± 4.48	0.788	55.16 ± 6.90	0.579		

AG, antegonion; CO, condyilion; J, jugale; L, left; NC, nasal cavity; PAC, conventional posterior anterior cephalometry; R, right; SD, standard deviation; ZA, zygomatic arch; ZF, zygomaticofrontal suture. The values given in bold are statistically significant.

Table 2 Comparison of measurements made in tilted, rotated and tipping positions with those made in central position on CBCT posteroanterior cephalograms separately for each landmark (in mm)

Position	Central		Tilt 10°		Tilt 20°		Central		Tilt 10°		Tilt 20°	
	R	R		R		L	L		L		L	
PAC/CBCT	Mean ± SD	Mean ± SD	p-value	Mean ± SD	p-value	Mean ± SD	Mean ± SD	p-value	Mean ± SD	Mean ± SD	p-value	Mean ± SD
AG	41.30 ± 4.87	40.92 ± 4.20	0.762	40.71 ± 4.57	0.588	40.25 ± 3.63	42.30 ± 3.31	0.027	42.47 ± 3.29	0.025		
J	30.10 ± 2.31	28.30 ± 2.32	0.032	28.21 ± 2.58	0.050	28.96 ± 2.35	29.05 ± 2.20	0.876	29.17 ± 1.51	0.787		
ZA	54.21 ± 1.46	54.03 ± 1.55	0.772	53.95 ± 2.02	0.736	53.27 ± 1.45	54.73 ± 1.72	0.082	54.79 ± 2.20	0.130		
NC	10.89 ± 1.25	10.31 ± 1.57	0.259	10.05 ± 1.16	0.070	11.04 ± 1.30	11.41 ± 0.55	0.405	11.63 ± 0.59	0.215		
ZF	50.43 ± 0.40	50.06 ± 0.59	0.032	49.94 ± 1.19	0.168	49.84 ± 0.46	49.95 ± 0.53	0.497	50.15 ± 0.95	0.248		
CO	54.22 ± 3.39	53.51 ± 1.79	0.536	52.09 ± 2.93	0.008	53.17 ± 3.04	53.35 ± 3.50	0.816	53.56 ± 4.07	0.744		
Position	Central	Rotation 10°	p-value	Rotation 20°	p-value	Central	Rotation 10°	p-value	Rotation 20°	p-value		
Side	R	R		R		L	L		L			
PAC/CBCT	Mean ± SD	Mean ± SD		Mean ± SD		Mean ± SD	Mean ± SD		Mean ± SD			
AG	41.30 ± 4.87	34.47 ± 4.48	0.000	27.54 ± 4.84	0.000	40.25 ± 3.63	49.27 ± 4.51	0.000	63.01 ± 5.63	0.000		
J	30.10 ± 2.31	25.70 ± 3.11	0.000	21.12 ± 3.82	0.000	28.96 ± 2.35	32.79 ± 2.11	0.010	41.97 ± 4.04	0.000		
ZA	54.21 ± 1.46	48.10 ± 2.29	0.000	34.26 ± 3.04	0.000	53.27 ± 1.45	57.93 ± 2.69	0.000	65.98 ± 5.09	0.000		
NC	10.89 ± 1.25	10.29 ± 1.86	0.224	9.34 ± 2.46	0.085	11.04 ± 1.30	12.07 ± 2.17	0.179	12.58 ± 2.27	0.157		
ZF	50.43 ± 0.40	48.10 ± 2.31	0.013	42.87 ± 3.54	0.000	49.84 ± 0.46	52.88 ± 4.33	0.044	57.39 ± 3.06	0.000		
CO	54.22 ± 3.39	42.03 ± 4.26	0.000	32.40 ± 6.10	0.000	53.17 ± 3.04	63.41 ± 5.96	0.000	79.19 ± 4.14	0.000		
Position	Central	Tip 10°	p-value	Tip 20°	p-value	Central	Tip 10°	p-value	Tip 20°	p-value		
Side	R	R		R		L	L		L			
PAC/CBCT	Mean ± SD	Mean ± SD		Mean ± SD		Mean ± SD	Mean ± SD		Mean ± SD			
AG	41.30 ± 4.87	42.52 ± 3.72	0.242	43.63 ± 5.50	0.075	40.25 ± 3.63	41.07 ± 2.00	0.463	42.85 ± 3.42	0.064		
J	30.10 ± 2.31	30.53 ± 1.43	0.537	30.74 ± 0.79	0.416	28.96 ± 2.35	29.07 ± 2.26	0.842	29.52 ± 3.34	0.484		
ZA	54.21 ± 1.46	54.37 ± 3.11	0.866	55.68 ± 3.53	0.181	53.27 ± 1.45	53.58 ± 3.13	0.817	55.32 ± 3.74	0.125		
NC	10.89 ± 1.25	11.31 ± 0.13	0.360	11.47 ± 0.58	0.197	11.04 ± 1.30	11.97 ± 1.05	0.149	11.98 ± 0.59	0.062		
ZF	50.43 ± 0.40	50.54 ± 0.94	0.663	50.76 ± 1.42	0.429	49.84 ± 0.46	49.84 ± 0.46	0.748	50.03 ± 0.78	0.551		
CO	54.22 ± 3.39	54.67 ± 5.28	0.639	55.16 ± 5.00	0.601	53.17 ± 3.04	53.48 ± 4.37	0.803	53.77 ± 4.17	0.688		

AG, antegonion; CO, condyilion; J, jugale; L, left; NC, nasal cavity; PAC/CBCT, the posterior anterior cephalograms were obtained from CBCT images; R, right; SD, standard deviation; ZA, zygomatic arch; ZF, zygomaticofrontal suture. The values given in bold are statistically significant.

multiple structures also inherent in conventional projection radiography.²⁵ The mean of SDs for measurements made on CBCT PA cephalograms was lower than that of conventional PA cephalograms. Therefore, CBCT PA cephalograms are probably more accurate than conventional PA cephalograms. The reason for this finding may be the statistically significant difference in identification of landmarks on conventional and CBCT cephalograms. Another reason is that in contrast to conventional radiographs, these ray sum images are without magnification and parallax distortion.²⁵ Since the CBCT PA cephalograms do not have magnification or parallax distortion (compared with conventional PA cephalograms), landmark identification and subsequent transverse measurements on CBCT PA cephalograms have higher accuracy.²⁵

Chen et al,¹² in their study, concluded that CBCT cephalograms were more reliable than conventional cephalograms for detection of landmarks. Their results were similar to our findings. Cattaneo et al²⁶ found no significant difference between measurements made on conventional radiographs and those made on CBCT cephalograms ($p > 0.05$). Their results were in contrast to ours. In conventional cephalometry, X-ray beams are not parallel. Thus, objects closer to the X-ray tube have higher magnification on the image. When 3D structures of the skull are visualized on a 2D detector, varying distances from the X-ray tube result in different sizes of landmarks on the image. However, 2D cephalograms synthesized of CBCT scans are built by adjusting the centre of projection at an infinite distance from the

Table 3 Comparison of measurements made in central position on conventional and CBCT posteroanterior cephalograms separately for each landmark (in mm)

Position	Central PAC		Central PAC/CBCT		Central PAC		Central PAC/CBCT	
	R	R		R	L	L		L
PAC	Mean ± SD	Mean ± SD	p-value	Mean ± SD	Mean ± SD	Mean ± SD	Mean ± SD	p-value
AG	39.46 ± 4.87	41.30 ± 4.87	0.008	41.72 ± 3.74	40.25 ± 3.63	41.72 ± 3.74	40.25 ± 3.63	0.127
J	28.24 ± 2.58	30.10 ± 2.31	0.030	28.98 ± 3.11	28.96 ± 2.35	28.98 ± 3.11	28.96 ± 2.35	0.985
ZA	53.65 ± 1.74	54.21 ± 1.46	0.084	54.52 ± 1.68	53.27 ± 1.45	54.52 ± 1.68	53.27 ± 1.45	0.104
NC	11.12 ± 1.51	10.89 ± 1.25	0.582	12.84 ± 2.29	11.04 ± 1.30	12.84 ± 2.29	11.04 ± 1.30	0.014
ZF	50.22 ± 1.11	50.43 ± 0.40	0.500	49.91 ± 1.04	49.84 ± 0.46	49.91 ± 1.04	49.84 ± 0.46	0.807
CO	52.57 ± 2.98	54.22 ± 3.39	0.241	54.25 ± 4.19	53.17 ± 3.04	54.25 ± 4.19	53.17 ± 3.04	0.407

AG, antegonion; CO, condyilion; J, jugale; L, left; NC, nasal cavity; PAC, posterior anterior cephalometry; PAC/CBCT, the posterior anterior cephalograms were obtained from CBCT images; R, right; SD, standard deviation; ZA, zygomatic arch; ZF, zygomaticofrontal suture. The values given in bold are statistically significant.

Table 4 The mean, confidence interval and significance of differences in the accuracy of measurements made in central position on conventional and CBCT posteroanterior cephalograms separately for each landmark (in mm)

Landmark	Number of repetition	Mean (SD)	Confidence interval 95%	Significant difference in accuracy
PAC-AG-R	1000	4.57	2.82–6.32	No difference
PAC/CBCT-AG-R	1000	4.60	3.17–6.03	
PAC-AG-L	1000	3.44	1.96–4.91	No difference
PAC/CBCT-AG-L	1000	3.33	1.55–5.11	
PAC-J-R	1000	2.40	1.56–3.24	No difference
PAC/CBCT-J-R	1000	2.14	1.24–3.02	
PAC-J-L	1000	3.88	1.64–4.12	No difference
PAC/CBCT-J-L	1000	2.18	1.33–3.03	
PAC-ZA-R	1000	1.63	1.12–2.14	No difference
PAC/CBCT-ZA-R	1000	1.35	0.80–1.93	
PAC-ZA-L	1000	1.57	1.06–2.08	No difference
PAC/CBCT-ZA-L	1000	1.36	0.78–1.93	
PAC-NC-R	1000	1.40	0.88–1.91	No difference
PAC/CBCT-NC-R	1000	1.17	0.78–1.55	
PAC-NC-L	1000	2.16	1.54–2.77	No difference
PAC/CBCT-NC-L	1000	1.18	0.45–1.91	
PAC-ZF-R	1000	1.03	0.53–1.53	No difference
PAC/CBCT-ZF-R	1000	0.38	0.24–1.52	
PAC-ZF-L	1000	0.97	0.50–1.44	No difference
PAC/CBCT-ZF-L	1000	0.43	0.29–0.56	
PAC-CO-R	1000	2.80	1.46–3.73	No difference
PAC/CBCT-CO-R	1000	3.13	1.70–4.57	
PAC-CO-L	1000	3.89	2.11–5.67	No difference
PAC/CBCT-CO-L	1000	2.84	1.85–3.84	

AG, antegonion; CO, condylian; J, jugale; NC, nasal cavity; SD, standard deviation; ZA, zygomatic arch; ZF, zygomaticofrontal suture.

projection plane; thus, parallel rays are simulated and magnification errors are non-existent. Thus, reliability of landmark identification is higher in CBCT cephalometry.¹² Also, CBCT cephalograms have higher contrast than conventional cephalograms, and

thus anatomical landmarks can be evaluated more easily and with higher accuracy.²⁷

In our study, the mean distances measured on CBCT PA cephalograms were greater than those measured on conventional PA cephalograms. Also, on both

Table 5 Comparison of measurements made in the right and left sides in 10° and 20° rotations compared with the central position on conventional and CBCT posteroanterior cephalograms separately for each landmark (in mm)

Landmark	Mean	SD	95% confidence interval of the difference		p-value
			Lower	Upper	
Right					
AG—Rotation 10	3.590	4.306	0.509	6.670	0.027
AG—Rotation 20	8.660	7.444	3.334	13.985	0.005
J—Rotation 10	3.590	4.012	0.719	6.460	0.020
J—Rotation 20	7.030	5.021	3.437	10.622	0.002
ZA—Rotation 10	3.520	3.530	0.994	6.045	0.012
ZA—Rotation 20	16.370	3.472	13.885	18.854	0.000
NC—Rotation 10	-0.680	2.199	-2.253	0.893	0.354
NC—Rotation 20	-1.080	2.839	-3.111	0.951	0.260
ZF—Rotation 10	1.130	2.585	-0.719	2.979	0.200
ZF—Rotation 20	6.110	3.829	3.370	8.849	0.001
CO—Rotation 10	6.940	7.287	1.726	12.153	0.015
CO—Rotation 20	12.040	7.384	6.757	17.322	0.001
Left					
AG—Rotation 10	-6.010	3.980	-8.857	-3.162	0.001
AG—Rotation 20	-16.190	6.539	-20.868	-11.511	0.000
J—Rotation 10	-2.600	5.983	-6.880	1.680	0.203
J—Rotation 20	-11.290	6.738	-16.110	-6.469	0.000
ZA—Rotation 10	-2.730	3.451	-5.199	-0.260	0.034
ZA—Rotation 20	-9.870	5.413	-13.742	-5.997	0.000
NC—Rotation 10	-0.950	2.540	-2.767	0.867	0.267
NC—Rotation 20	-1.140	3.696	-3.783	1.503	0.355
ZF—Rotation 10	-2.310	4.476	-5.512	0.892	0.137
ZF—Rotation 20	-6.650	3.642	-9.255	-4.044	0.000
CO—Rotation 10	-3.350	7.578	-8.771	2.071	0.196
CO—Rotation 20	-15.590	8.319	-21.541	-9.638	0.000

AG, antegonion; CO, condylian; J, jugale; NC, nasal cavity; SD, standard deviation; ZA, zygomatic arch; ZF, zygomaticofrontal suture.

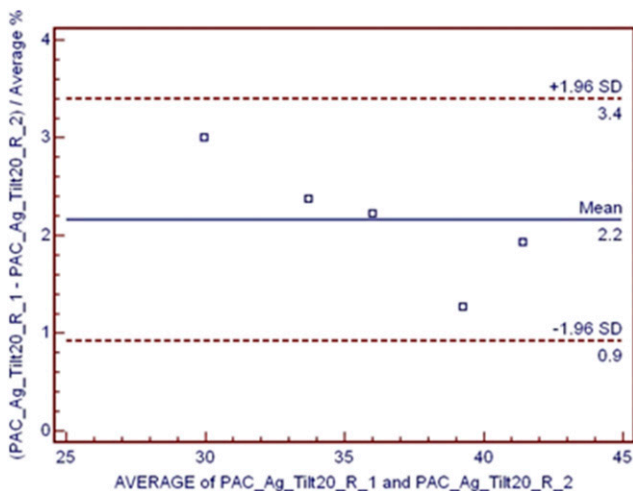


Figure 10 High interobserver agreement in antegonion measurements in 20° tilted position in the right side on conventional posteroanterior cephalogram. SD, standard deviation.

conventional and CBCT PA cephalograms, significant changes in different positions (compared with the central position) were mainly related to AG, condyilion and zygomaticofrontal suture landmarks. Oz *et al*²⁴ concluded that identification and measurement of landmarks on curved surfaces of the skull such as AG and condyilion on CBCT PA cephalograms are subject to more errors and alterations than other landmarks. Their findings were in agreement with ours. The reason is, on PA cephalograms, landmarks are located at varying distances from the midline and those farther from the midline are subject to more alterations than those closer to the midline.¹⁵

In the present study, we found that the rotated position affected the mean values more than the tilted position. The mean distances measured in tipped position were the closest to the mean values measured in central position. Hassan *et al*¹⁵ discussed that linear measurements are

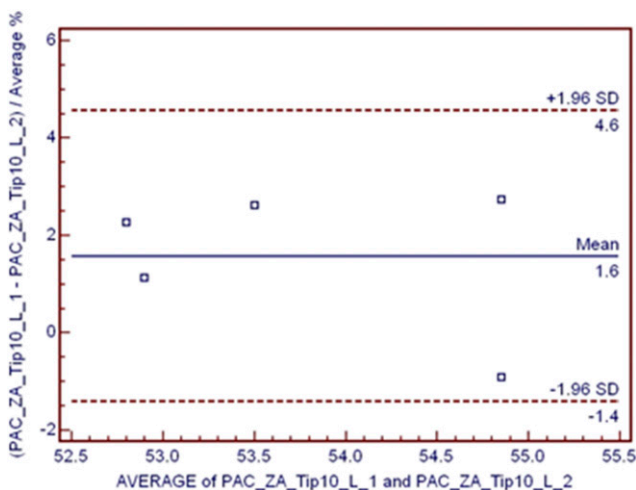


Figure 11 Low interobserver agreement in zygomatic arch measurements in the 10° tilted position in the left side on conventional posteroanterior cephalogram. SD, standard deviation.

influenced by two factors, namely errors in patient positioning and location of anatomical landmarks. Moreover, Hassan *et al*¹⁵ showed that rotation of the skull (relative to the central position) caused more than 10-mm difference in measurement of transverse distances. It means that CBCT scans are sensitive even to the slightest changes in patient position. Linear measurements made on 2D lateral and CBCT PA cephalograms are also sensitive to the slightest changes in patient head position. These findings were in accordance with ours. Furthermore, van Vlijmen *et al*¹⁴ compared conventional and CBCT lateral cephalograms and reported a significant difference between the two ($p < 0.05$). Their results were in line with our findings. Also van Vlijmen *et al* reported that head tilting in both conventional and CBCT lateral cephalometry had no effect on the accuracy of linear or angular measurements because all these points would move in the same direction.¹⁴ Their results were in contrast to our findings. Reduction in accuracy of landmark identification as the result of head rotation may be attributed to superimposition of skull structures. Structures located farther from the rotational axis move to a greater extent than those closer to the rotational axis. Also, structures located opposite to the direction of rotation move towards the other side. In some cases, rotation of the skull results in superimposition of structures, which decreases the clarity of landmarks and increases the range of diagnostic errors. By rotating the head towards the left or right side, landmarks in the two sides of the skull are affected differently. In some cases, rotation of the skull results in movement of structures towards the area with less superimposition, and identification of structures is enhanced as such. By rotation of the skull around the mid-sagittal axis, horizontal relations are affected, but vertical relations remain unchanged; this complicates the assessment of asymmetry relative to the midline.²⁸ In the tipped position, the mean distances measured were greater than those measured in the central position (had an ascending trend). This finding was in agreement with the results of Major *et al*,²⁸ because the tipped position (rotation around a transverse axis) affects the relationship of landmarks in the vertical (and not horizontal) dimension, since landmarks on both sides of the skull move to the same extent. In our study, significant differences were noted for most landmarks in measurements made on conventional and CBCT PA cephalograms in 10° and 20° rotations compared with the central position at both sides. This controversy in the results of the two studies is attributed to the difference in PA and lateral cephalometry techniques. Rotation affects the measurement of distances made on CBCT PA cephalograms more than that on conventional cephalograms. Van Vlijmen *et al*² reported that the difference in the mean measurements made on conventional and CBCT PA cephalograms was statistically significant ($p < 0.001$). Their findings were almost similar to ours. No statistically significant difference was noted in the interobserver agreements between the two methods of conventional and CBCT PA cephalometry. In the

conventional PA cephalometry, the highest (99%) and the lowest (71%) agreement belonged to AG and zygomatic arch landmarks, respectively. In the CBCT PA cephalometry, the highest (99%) and the lowest (72%) agreement belonged to J and zygomatico-frontal suture landmarks, respectively.

This study was conducted on dry human skulls, and therefore it had limitations compared with *in vivo* studies. Future studies with the use of phantoms are

required to simulate soft tissues to obtain more accurate results.

In conclusion, the CBCT PA cephalometry is more accurate than the conventional PA cephalometry. On both conventional and CBCT PA cephalograms, landmarks farther from the midline are subject to more changes than those closer to the midline. Rotation of the head affects the measurements made on CBCT PA cephalograms more than those made on conventional PA cephalograms.

References

- Damstra J, Fourie Z, Ren Y. Evaluation and comparison of postero-anterior cephalograms and cone-beam computed tomography images for the detection of mandibular asymmetry. *Eur J Orthod* 2013; **35**: 45–50.
- van Vlijmen OJ, Maal TJ, Bergé SJ, Bronkhorst EM, Katsaros C, Kuijpers-Jagtman AM. A comparison of frontal radiographs obtained from cone beam CT scans and conventional frontal radiographs of human skulls. *Int J Oral Maxillofac Surg* 2009; **38**: 773–8. doi: <https://doi.org/10.1016/j.ijom.2009.02.024>
- Betts NJ, Vanarsdall RL, Barber HD, Higgins-Baerber K, Fonesca RJ. Diagnosis and treatment of transverse maxillary deficiency. *Int J Adult Orthodon Orthognath Surg* 1995; **10**: 75–96.
- Caple JM, Stephan CN, Gregory LS, MacGregor DM. Effect of head position on facial soft tissue depth measurements obtained using computed tomography. *J Forensic Sci* 2016; **61**: 147–52. doi: <https://doi.org/10.1111/1556-4029.12896>
- Poleti ML, Fernandes TM, Pagin O, Moretti MR, Rubira-Bullen IR. Analysis of linear measurements on 3D surface models using CBCT data segmentation obtained by automatic standard pre-set thresholds in two segmentation software programs: an *in vitro* study. *Clin Oral Investig* 2016; **20**: 179–85. doi: <https://doi.org/10.1007/s00784-015-1485-5>
- Leonardi R, Annunziata A, Caltabiano M. Landmark identification error in posteroanterior cephalometric radiography: a systematic review. *Angle Orthod* 2008; **78**: 761–5.
- Periago DR, Scarfe WC, Moshiri M, Scheetz JP, Silveria AM, Farman AG. Linear accuracy and reliability of cone beam CT derived 3-dimensional images constructed using an orthodontic volumetric rendering program. *Angle Orthod* 2008; **78**: 387–95.
- Malkoc S, Sari Z, Usumez S, Koyuturk AE. The effect head rotation cephalometric radiographs. *Eur J Orthod* 2005; **27**: 315–21. doi: <https://doi.org/10.1093/ejo/cjh098>
- Betts NJ, Sturtz DH, Aldrich DA. Treatment of transverse (width) discrepancies in patients who require isolated mandibular surgery: the case for maxillary expansion. *J Oral Maxillofac Surg* 2004; **62**: 361–4.
- Lee HJ, Lee S, Lee EJ, Song IJ, Kang BC, Lee JS, et al. A comparative study of the deviation of the menton on postero-anterior cephalograms and three-dimensional computed tomography. *Imaging Sci Dent* 2016; **46**: 33–8.
- Kim MS, Lee EJ, Song IJ, Lee JS, Kang BC, Yoon SJ. The location of midfacial landmarks according to the method of establishing the midsagittal reference plane in three-dimensional computed tomography analysis of facial asymmetry. *Imaging Sci Dent* 2015; **45**: 227–32.
- Chen MH, Chang JZ, Kok SH, Chen YJ, Huang YD, Cheng KY, et al. Intraobserver reliability of landmark identification in cone-beam computed tomography-synthesized two-dimensional cephalograms versus conventional cephalometric radiography: a preliminary study. *J Dent Sci* 2014; **9**: 56–62.
- Ludlow JB, Gubler M, Cevidanes L, Mol A. Precision of cephalometric landmark identification: cone-beam computed tomography vs conventional cephalometric views. *Am J Orthod Dentofacial Orthop* 2009; **136**: 312.e1–10.
- van Vlijmen OJ, Bergé SJ, Swennen GR, Bronkhorst EM, Katsaros C, Kuijpers-Jagtman AM. Comparison of cephalometric radiographs obtained from cone-beam computed tomography scans and conventional radiographs. *J Oral Maxillofac Surg* 2009; **67**: 92–7. doi: <https://doi.org/10.1016/j.joms.2008.04.025>
- Hassan B, van der Stelt P, Sanderink G. Accuracy of three-dimensional measurements obtained from cone beam computed tomography surface-rendered images for cephalometric analysis: influence of patient scanning position. *Eur J Orthod* 2009; **31**: 129–34.
- Sato H, Ohki M, Kitamori H. A method for quantifying positional change of the condyle on lateral tomograms by means of digital subtraction. *J Oral Rehabil* 1998; **25**: 448–55. doi: <https://doi.org/10.1046/j.1365-2842.1998.00252.x>
- Paul PE, Barbenel JC, Walker FS, Khambay BS, Moos KF, Ayoub AF. Evaluation of an improved orthognathic articulator system. 2. Accuracy of occlusal wafers. *Int J Oral Maxillofac Surg* 2012; **41**: 155–9.
- Ludlow JB, Davies-Ludlow LE, Brooks SL, Howerton WB. Dosimetry of 3 CBCT devices for oral and maxillofacial radiology: CB Mercury, NewTom 3G and i-CAT. *Dentomaxillofac Radiol* 2006; **35**: 219–26.
- Greiner M, Greiner A, Hirschfelder U. Variance of landmarks in digital evaluation: comparison between CT-based and conventional digital lateral cephalometric radiographs. [In German.] *J Orofac Orthop* 2007; **68**: 290–8.
- Kumar V, Ludlow JB, Mol A, Cevidanes L. Comparison of conventional and cone beam CT synthesized cephalograms. *Dentomaxillofac Radiol* 2007; **36**: 263–9. doi: <https://doi.org/10.1259/dmfr/98032356>
- Major PW, Johnson DE, Hesse KL, Glover KE. Landmark identification error in posterior anterior cephalometrics. *Angle Orthod* 1994; **64**: 447–54.
- El-Mangoury NH, Shaheen SI, Mostafa YA. Landmark identification in computerized posteroanterior cephalometrics. *Am J Orthod Dentofacial Orthop* 1987; **91**: 57–61.
- Schlicher W, Nielsen I, Huang JC, Maki K, Hatcher DC, Miller AJ. Consistency and precision of landmark identification in three dimensional cone beam computed tomograph scans. *Eur J Orthod* 2012; **34**: 263–75.
- Oz U, Orhan K, Abe N. Comparison of linear and angular measurements using two-dimensional conventional methods and three-dimensional cone beam CT images reconstructed from a volumetric rendering program *in vivo*. *Dentomaxillofac Radiol* 2011; **40**: 492–500.
- White SC, Pharoah MJ, eds. *Oral radiology: principles and interpretation*. 6th edn. St. Louis, MO: Mosby; 2014.
- Cattaneo PM, Bloch CB, Calmar D, Hjortshøj M, Melsen B. Comparison between conventional and cone-beam computed tomography-generated cephalograms. *Am J Orthod Dentofacial Orthop* 2008; **134**: 798–802.
- Liedke GS, Delamare EL, Vizzotto MB, da Silveira HL, Prietsch JR, Dutra V, et al. Comparative study between conventional and cone beam CT-synthesized half and total skull cephalograms. *Dentomaxillofac Radiol* 2012; **41**: 136–42. doi: <https://doi.org/10.1259/dmfr/22287302>
- Major PW, Johnson DE, Hesse KL, Glover KE. Effect of head orientation on posterior anterior cephalometric landmark identification. *Angle Orthod* 1996; **66**: 51–60.